
Integral Bulge Forming Method for Soccer Ball-Shaped Tank Using Symmetrical Preformed Box Consisting of Plate Parts

Yang Jing¹, Jingchao Guan¹, Chenghai Kong², Wei Zhao³, Nobuyuki Gomi¹, Xilu Zhao^{1,*}

¹Department of Mechanical, Saitama Institute of Technology, Saitama, Japan

²Topy Industries Ltd, Aichi, Japan

³Weichai Global Axis Technology Co., Ltd, Tokyo, Japan

Email address:

keiyou1012@gmail.com (Yang Jing), guanjingchao123@gmail.com (Jingchao Guan), kongchenghai@gmail.com (Chenghai Kong), shunsuke0390@gmail.com (Wei Zhao), n_gomi@sit.ac.jp (Nobuyuki Gomi), zhaoxilu@sit.ac.jp (Xilu Zhao)

*Corresponding author

To cite this article:

Yang Jing, Jingchao Guan, Chenghai Kong, Wei Zhao, Nobuyuki Gomi, Xilu Zhao. Integral Bulge Forming Method for Soccer Ball-Shaped Tank Using Symmetrical Preformed Box Consisting of Plate Parts. *American Journal of Mechanics and Applications*. Vol. 10, No. 2, 2022, pp. 16-24. doi: 10.11648/j.ajma.20221002.11

Received: September 24, 2022; Accepted: October 21, 2022; Published: October 28, 2022

Abstract: This study proposes an integral hydro-bulge forming method for a soccer ball-shaped tank to improve the manufacturing problem of conventional spherical tanks. By cutting the hexagonal and pentagonal parts from the flat steel plate and welding them along the sides of each part, a closed polyhedral box is created according to the composition of a soccer ball. Subsequently, pressure is applied with water into the closed polyhedral box, and the expansion force generated from the inside to the outside is used to form a soccer ball-shaped spherical tank. For verification, we simulate the bulge forming process of the soccer ball-shaped tank using the fine element method (FEM) analysis to confirm the analysis results of the stress and plate thickness distribution of the spherical tank created, and the soccer ball-shaped tank is then actually formed using the proposed manufacturing method. The forming performance and effectiveness of the integral hydro-bulge forming method is verified. The roundness of the actually formed soccer ball-shaped spherical tank with a diameter of 500 mm is 2.36 mm, which indicates high forming accuracy. A design formula $a=0.4R$ for regular hexagonal and regular pentagonal plate parts was derived. In the actual forming experiment, a plate part with a side length of 100 mm was designed with a target radius of 250 mm. The measured radius of the actually formed spherical tank was 249.26 mm, and the accuracy of the derived design formula was verified.

Keywords: Spherical Tank, Integral Hydro Forming, Thin-Walled Tank, Steel Plate Press Forming, Forming by Water Pressure

1. Introduction

Spherical tanks are widely used to store water and various industrial gases owing to their ideal shape for internal pressure. The design and manufacturing issues of spherical tanks are important [1-5].

A spherical tank is designed by considering that the symmetrical structure is the most rational for loads that are originally symmetrical, and the deformation, stress distribution, and buckling performance of spherical tanks have been investigated [6-8]. Recently, with the development of fine element method (FEM) analysis technology, numerous analysis results for spherical tanks have been

published. The mechanical properties of spherical tanks have gradually been elucidated [9-11].

However, owing to the large size of spherical tanks and their relatively small relative plate thickness, several problems limit their design and manufacturing. An important issue is the processing of a spherical tank with a simple method, at a low cost and with good shape accuracy [12-15].

The manufacturing process of a conventional spherical tank involves processing in almost two stages. First, according to the shape data of the curved part obtained by dividing the surface of the spherical tank, thin steel plate parts are individually formed into curved shapes by the sheet metal press method at the processing factory. Next, multiple

positioning jigs are installed along the latitude and longitude lines of the spherical tank at the construction site, and the thin curved steel plate parts are welded in order. Finally, the positioning jig is removed to obtain a spherical tank [16-19].

To overcome these problems, an integrated hydro-bulge forming method has been developed, and several studies have addressed it. In the integrated hydro-bulge forming method, a sealed thin-walled pre-box is fabricated. Next, by applying water pressure to the inside, the pre-box is inflated to form a spherical tank. However, the shape of the pre-box contains asymmetrical elements, and the roundness of the molded spherical tank is relatively low [20-22]. Because the curved parts are included in the pre-box, of the method has a relatively low forming accuracy. Therefore, an inexpensive and simple forming method must be developed.

The manufacturing process is complicated, with two main problems. One is the need for dies to stamp curved thin steel plate parts at processing plants. Because of the spring-back phenomenon that occurs when forming thin steel plate parts with three-dimensional curved surfaces, ensuring a high processing shape accuracy is difficult. The other problem concerns the cost of preparing a large positioning jig at a construction site and difficulty in ensuring the accuracy of the shape of the welded spherical tank.

In this study, we proposed a ball-shaped tank and an integrated hydro-bulge molding method to process it. A soccer ball-shaped tank was decomposed into regular hexagonal and pentagonal thin steel plate parts, and the relational formula between the diameter of the formed spherical tank and shape parameters of the basic constituent parts were derived. A calculation formula for the hydraulic pressure required for hydro-bulge formation was derived, and the spring-back problem after forming was examined. For verification, the FEM analysis method was used to simulate the hydro-bulging process of a soccer ball-shaped tank, and the feasibility of this processing method was confirmed using the analysis results of the stress and plate thickness distribution of the spherical tank formed. Hydro bulge forming experiments were conducted to

verify the formation performance and effectiveness of the proposed forming method.

2. Materials and Methods

2.1. Soccer Ball-Shaped Spherical Tank

A conventional spherical tank was manufactured, as shown in Figure 1. First, in the factory, curved thin steel plate parts were individually processed by the sheet metal press method using punches and forming dies. Subsequently, at the construction site, a spherical tank was obtained by sequentially welding thin curved steel plate parts using a circular ring-shaped positioning jig. This manufacturing method requires processing time and cost, and ensuring the shape accuracy of the processed spherical tank is difficult.

To address these processing problems, we proposed a soccer ball-shaped tank and integrated hydro-bulge molding method to process it. First, as shown in Figure 2, regular hexagons (20 pieces) and regular pentagons (12 pieces) with equal side lengths were cut from a flat plate using a laser processing machine. Following the shape of a soccer ball, each part was welded along the sides to construct a soccer ball-shaped polygonal cubic box. Subsequently, a spherical tank was obtained by applying water pressure to the inside of a sealed polygonal cubic box and forming a bulge from the inside by the expansion force of the water pressure.

The proposed integrated hydro-bulge forming method has two major advantages over conventional processing methods. First, because the welded parts can be cut directly from a flat thin steel plate, sheet metal press forming using dies is not required. Next, welding along the sides of the hexagons and pentagons results in a natural geometric soccer ball shape; thus, jig alignment during welding is unnecessary. Furthermore, as the expansion force of the water pressure in the polygonal cube box becomes completely symmetric, the shape accuracy of the hydro-bulged spherical tank can be distributed uniformly.

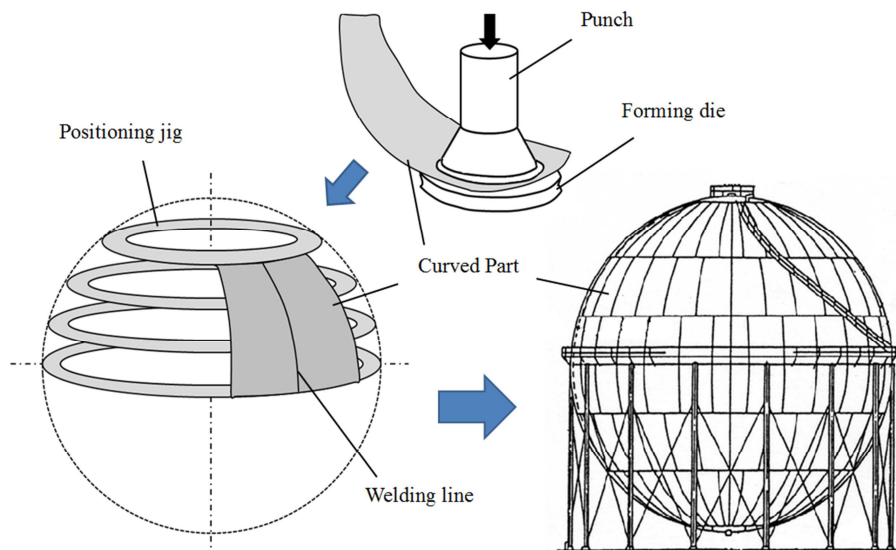


Figure 1. Conventional spherical tank manufacturing method.

2.2. Basic Component Plate Parts

The only design parameter for the polygonal cubic box shown in Figure 2 is the side length a ; to design the basic component plate part of this forming method, the side length a should be calculated from the radius R of the spherical tank.

To facilitate the hydro-bulging of a spherical tank, forming a regular polyhedron that resembles a spherical shape as much as possible is considered advantageous. Geometrically, the five types of regular polyhedrons include: tetrahedrons, hexahedrons, octahedrons, dodecahedrons, and icosahedrons. Among these, the regular icosahedron with the largest number of faces was the focus of this study. As shown in Figure 3(a), the regular icosahedron consists of 20 equilateral triangles, and five equilateral triangles meet at 12 vertices.

If we divide the sides of the regular icosahedron into three equal parts and cut the vertices through the trisecting points, as shown by the dotted lines in Figure 3(b), we obtain a soccer-ball-shaped polygonal cubic box, as shown in Figure 2. The part enclosed by the dotted lines in Figure 3(b) corresponds to the black regular pentagon in Figure 2, and the shaded part in Figure 3(b) corresponds to the regular hexagon in Figure 2.

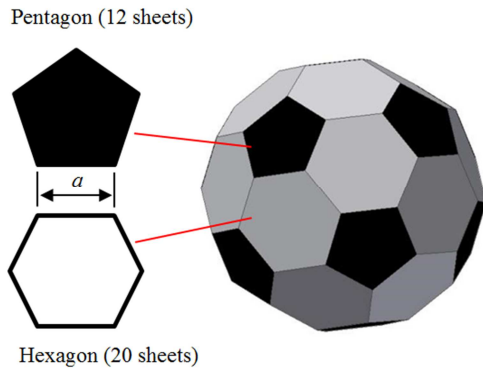


Figure 2. Polygonal cube box composed of hexagonal and pentagonal parts.

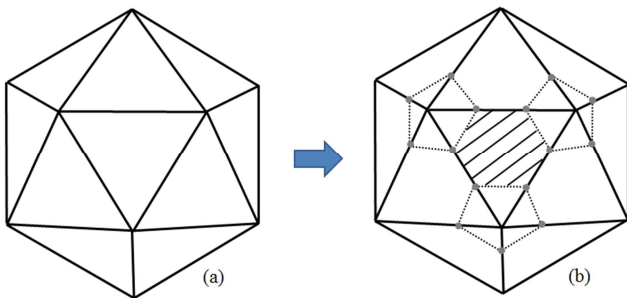


Figure 3. Regular icosahedron and soccer ball-shaped polygonal cubic box.

Assuming that the side length of the regular icosahedron shown in Figure 3(a) is $3a$, the distance from the inner center of the regular icosahedron to the center point of the surface regular triangle is expressed as follows.

$$R_{in} = \frac{3\sqrt{3} + \sqrt{15}}{12} (3a) = \frac{3\sqrt{3} + \sqrt{15}}{4} a \tag{1}$$

Figure 4 shows a regular hexagon separated from the surface of the soccer-ball-shaped polygonal cubic box shown in Figure 3(b). Herein, o is assumed to be the center of the soccer ball-shaped polygonal cube, and the center point of the formed spherical tank is assumed to not change; o' is the center point of the equilateral triangle; and R is the distance from the center point of the cube to the apex. If the bulging stops when the sphere is formed, then R may equal the radius of the formed spherical tank. As distance R_{in} does not change, the right triangle $oo'm$ in Figure 4 provides the following relation.

$$R = \sqrt{R_{in}^2 + a^2} \tag{2}$$

By substituting Equation (1) into equation (2), the design equation for the basic component plate parts is obtained as follows.

$$a = \frac{4R}{\sqrt{(3\sqrt{3} + \sqrt{15})^2 + 4^2}} = 0.4R \tag{3}$$

When forming a spherical tank, if the radius R of the spherical tank is determined, the side length a of the regular hexagonal and pentagonal flat plate parts can be obtained using Equation (3).

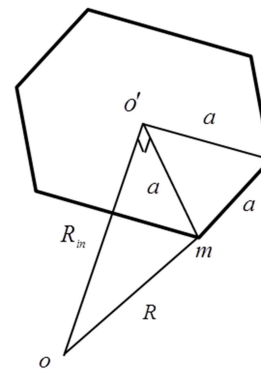


Figure 4. Relationship between the radius of the spherical tank and side lengths of the plate parts.

3. Results

3.1. Confirming the Forming Performance Using FEM

To confirm the forming performance, FEM was used to analyze the hydro-bulge forming process, wherein water pressure was applied to the welded polygonal cubic box. The side lengths of the regular hexagon and pentagon shown in Figure 2 were determined to be 100 mm.

Figure 5 illustrates the analysis model. Quadrilateral and triangular elements, with an average side length of 5 mm, were used. The plate thickness was 1 mm; Young's modulus of the stainless SUS304 material was 193 GPa and Poisson's ratio was 0.3.

Figure 6 shows the stress-strain relationship of the

materials used for plastic deformation. For the hydro-bulge forming analysis, only one node was fixed and the other nodes were free. The maximum internal water pressure for molding was set to 2.3 MPa.



Figure 5. Analysis model of free bulge forming process.

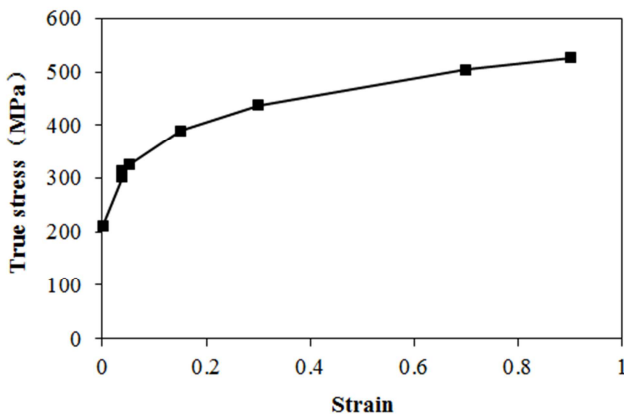


Figure 6. Stress-strain relationship graph.

Figures 7 and 8 show the von Mises stress and sheet thickness distributions, respectively, after the formation obtained via analysis. Figures 7 and 8 confirms that the hydro-bulge formation became uniform, and a smooth spherical tank surface was obtained because the internal water pressure was completely symmetrical.

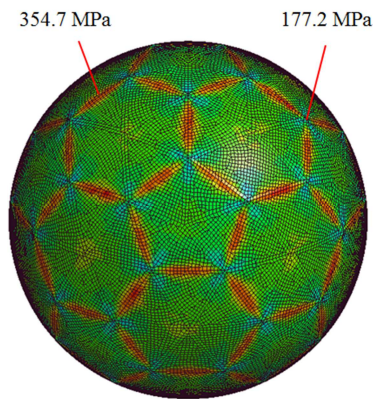


Figure 7. Results of stress distribution.

According to the stress distribution results in Figure 7, the maximum stress is distributed along the weld line, which is considered to be caused by the bending stress occurring in the linear weld line. The maximum and minimum von Mises stress were 354.7 and 177.2 MPa, respectively.

Based on the results of the plate thickness distribution in Figure 8, the plate thickness before formation was 1.0 mm,

but the overall thickness tended to be thinner. The central part of the regular hexagon was the thinnest, with a plate thickness of 0.963 mm and plate thickness reduction rate of 3.7%. The thickness reduction in the central part of the regular pentagon was moderated to a thickness of 0.971 mm and thickness reduction rate of 2.9%. The thickness reduction was smallest at the intersection of a regular hexagon and pentagon, with a thickness of 0.997 mm and thickness reduction rate of 0.3%.

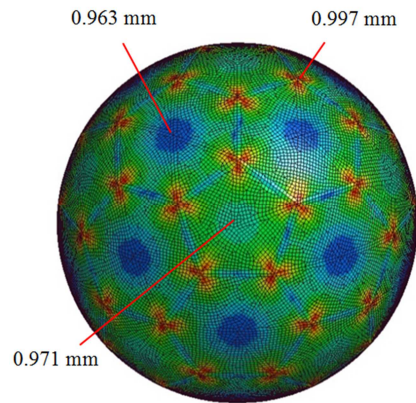


Figure 8. Results of thickness distribution.

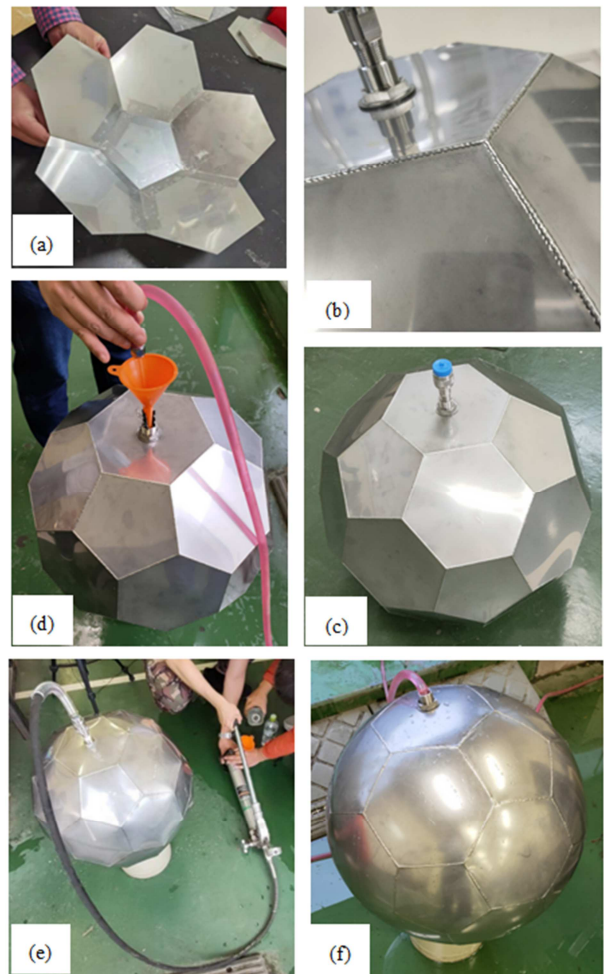


Figure 9. Bulge formation process of soccer ball-shaped tank.

The hydro-bulge forming method was primarily used to form regular hexagonal and pentagonal flat plate parts into curved surfaces, straight weld lines into curves, and polygonal cube boxes into spheres. Because the increase in the internal volume was relatively small, the maximum sheet thickness reduction rate after formation was only approximately 3.7%, which is considerably smaller than the plastic deformation limit of stainless-steel sheets. Therefore, forming a spherical tank using the hydro-bulge forming method can be accomplished normally without cracks.

3.2. Formation Experiment

Following the procedure shown in Figure 9, we conducted a formation experiment on a soccer ball-shaped spherical tank using the hydro-bulge forming method. As in the previous section, regular hexagonal and pentagonal thin plate parts with side lengths of 100 mm were used, and the material was stainless steel SUS304, with a plate thickness of 1 mm.

First, we cut out 20 regular hexagons and 12 pentagons using a laser processing machine. As shown in Figure 9(a), each flat plate part was temporarily fixed with gum tape in the shape of a soccer ball. If parts are joined without gaps, a polygonal cube box is obtained that is naturally sealed geometrically.

As shown in Figure 9(b), tungsten inert gas (TIG) welding was performed along the sides of each plate. A bulkhead socket was attached to the center of a hexagonal plate to apply water pressure inside. Consequently, a polygonal cubic box was created, as shown in Figure 9(c).

Furthermore, as shown in Figure 9(d), the polygonal cubic box was filled with water through the bulkhead socket. Using a manual hydraulic pump, water pressure was applied to the polygonal cube box, as shown in Figure 9(e), until it became a sphere.

Finally, as shown in Figure 9(f), the water was completely discharged from the inside to obtain a soccer ball-shaped tank.

3.3. Measurement of Forming Accuracy

The measurement system shown in Figure 10 was used to measure the roundness of the soccer ball-shaped tank formed using the hydro-bulge method. The external dimensions of the molded soccer-ball-shaped tank were measured using a camera stand, rotary table, and laser displacement meter (OPTEX CD22-35VM12, measurement accuracy ± 0.01 mm).

The spherical tank was fixed on a rotary table, as shown in Figure 10. The rotation angle of the spherical tank could be measured accurately by turning the handle of the rotary table.

The height from the pedestal to the laser displacement meter was measured by moving the horizontal beam of the stand up and down. A laser displacement meter was attached to the tip of the horizontal beam of the stand. This enabled us to measure the distance from the laser displacement meter to the surface of the spherical tank.

The height of the laser displacement meter, rotation angle of the rotary table, and distance from the laser displacement meter were measured, and coordinate conversion was performed to obtain the 3D coordinate values of the sample points on the surface of the spherical tank.

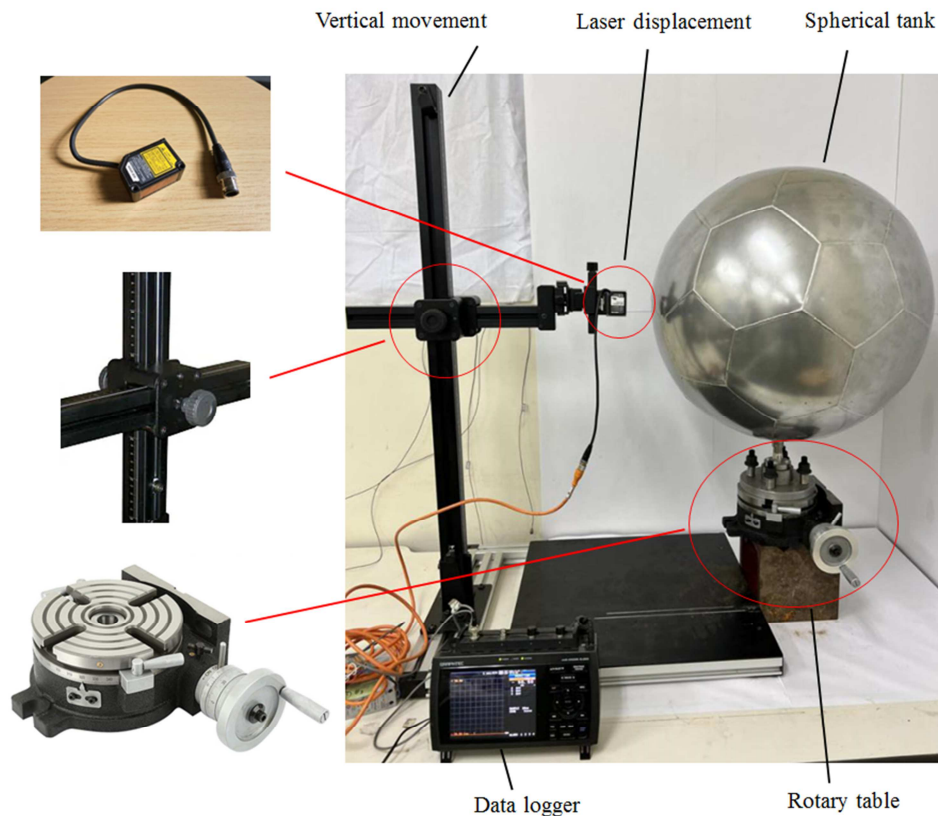


Figure 10. Measurement of processing accuracy of formed spherical tank.

As shown in Figure 11, a soccer-ball-shaped tank was obtained with seven cross sections at intervals of 30 mm in the vertical direction centered on the central section L0. For each cross section, 72 measurement sample points were taken

at intervals of 5° in the circumferential direction. Figure 12 shows the measurement results of the sampling points of the measured central cross-section.

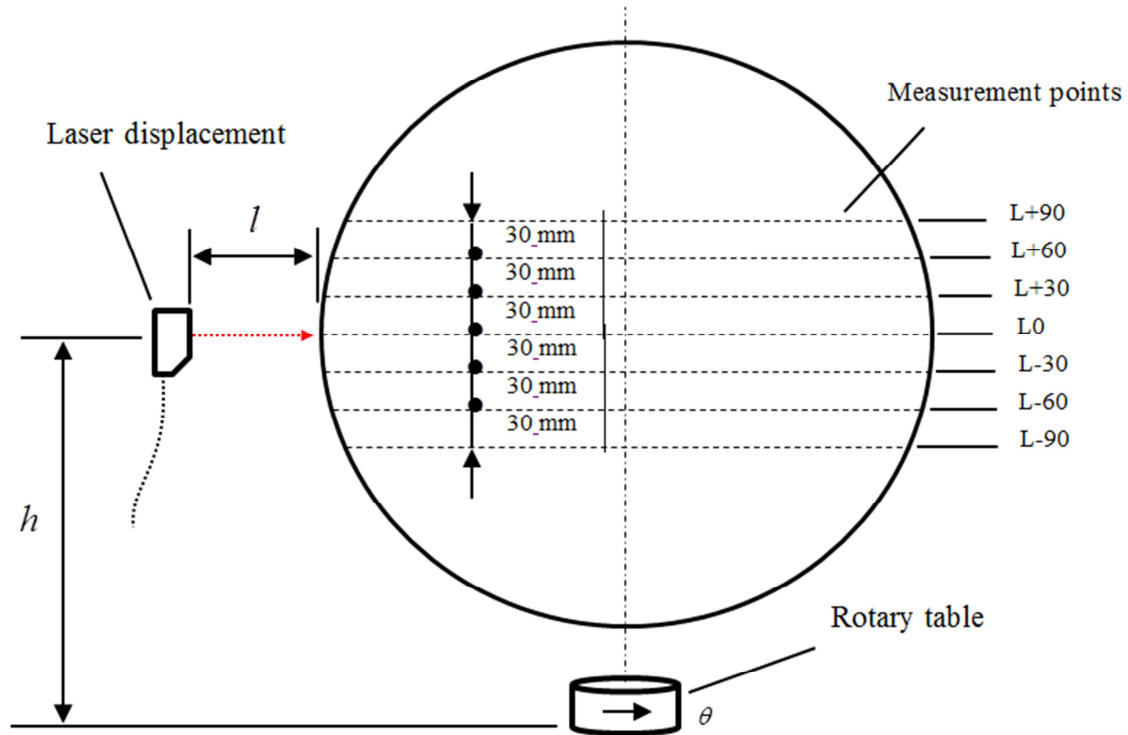


Figure 11. Measurement sample points and parameters of formed spherical tank.

Figure 12(a) shows the roundness comparison results calculated using the measurement coordinates of the sampling points in each cross section. The roundness of the seven cross-sections of the formed soccer ball-shaped tank were found to vary owing to factors, such as plate assembly errors and welding deformation. The circularity of the center section L0 was the smallest at 2.36 mm, and the average value of the circularity of the seven cross-sections was 3.21 mm. Because the roundness of a spherical tank with a diameter of approximately 500 mm is small, the processing accuracy is considered good.

Figures 12(b)–(h) show the measurement results of the sampling points in the seven cross-sections. The dotted red line indicates the coordinate position of the sampling point, and the solid blue line indicates the true circle in this cross section. The coordinates of the center of the circle were obtained by averaging the coordinate values of the 72 sampling points along the circumference. The radius values at the 72 sampling points were calculated, and the average radius was taken as the measured radius value of the circle in this cross section.

Figure 12(b) shows the measurement results for the central section L0. The measured sampling points were uniformly located on the circumference, and the formation quality represented by the circle was good, with an average radius of

249.26 mm.

Figures 12(c)–(e) show the measurement results of three cross-sections taken at 30 mm intervals downward from the center section of the spherical tank. The measured sampling points were uniformly located on the circumference. The average radii of the circumference at cross sections L+30, L+60, and L+90 were 246.18, 239.81, and 229.58 mm, respectively.

Figures 12(f)–(h) show the measurement results of three cross-sections taken at 30 mm intervals upward from the center section of the spherical tank. Similar to the measurement results in the downward direction, the measured sampling points were uniformly positioned on the circumference. The average radii of the circumference at cross sections L-30, L-60, and L-90 were 246.35, 240.76, and 231.47 mm, respectively.

From the measurement results in Figure 12, the spherical tank processed using the Integral Hydro Bulging Forming Method proposed in this paper has higher shape accuracy than the conventional method of welding pre-processed curved parts. The main reason for the high shape accuracy is that the internal water pressure is completely axially symmetrical, and the spherical tank is formed by uniformly applying the water pressure load.

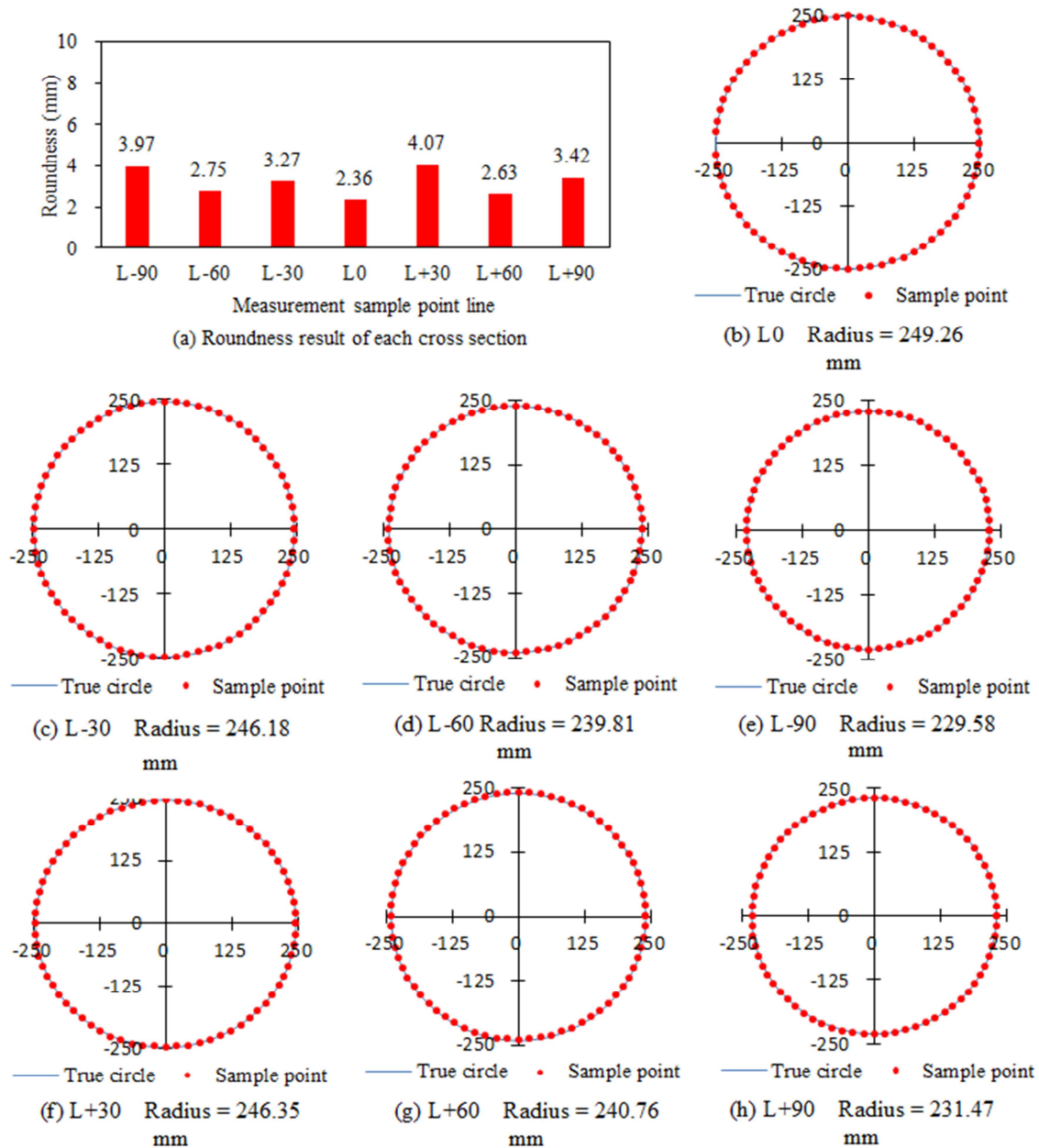


Figure 12. Measurement results of formed soccer ball-shaped tank.

4. Discussion

4.1. Validity of Design Equation (3)

For practical applications of the proposed method, the side lengths of the regular hexagonal and pentagonal plate parts from the radius of the spherical tank must be determined. To solve this problem, we derived design equation (3).

Here, the validity of design equation (3) was confirmed using the measurement results of the molded soccer ball-shaped tank discussed in the previous section.

Setting the side length a to 100 mm of the regular hexagonal and pentagonal plates used in the study into design equation (3), the resulting spherical tank radius d is 250 mm.

Moreover, the average radius of the formed spherical tank

was determined to be 249.26 mm from the measurement results of the central section L0 in Figure 12(b).

Comparing the two results, the error was found to be 0.29%, thereby verifying the validity of designing the basic component plate parts using design equation (3).

Because the only parameter for designing regular hexagonal and regular pentagonal plate parts was the side length, the formation process design could be completed by calculating the side length from the radius of the spherical tank using design equation (3).

4.2. Water Pressure

For examination, the spherical tank was cut in half, as shown in Figure 13, and the following equation was obtained from the equilibrium relationship between the internal water

pressure and tensile stress on the side wall.

$$\sigma = \frac{PR}{2t} \quad (4)$$

where R is the radius of the spherical tank; and t is the plate thickness. When applying internal water pressure, the stress acting on the sidewall of the spherical tank began to deform the plastic as it reached the yield stress of the material. The internal water pressure required was calculated using the following equation.

$$P = \frac{2t\sigma_s}{R} \quad (5)$$

Considering the effects of the work hardening of the material, the actual water pressure required for hydro-bulging should be set to approximately 10% higher than the value at the onset of plastic deformation, calculated using Equation (5).

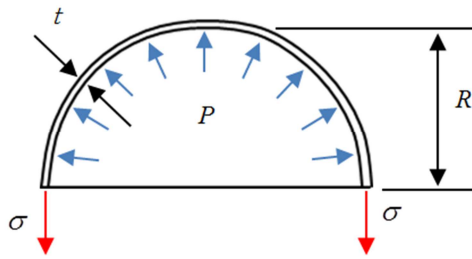


Figure 13. Internal hydraulic pressure and tensile stress during the bulging forming.

The formation experiment in the previous section revealed a yield stress of 255 MPa with the stainless steel SUS304 plate, plate thickness of 1.0 mm, and radius of the spherical tank of 250 mm. These values were substituted into Equation (5). Thus, the water pressure at which the plastic deformation begins could be calculated using the following equation.

$$P = \frac{2 \times 0.001 \times 255}{0.25} = 2.04 \text{ MPa} \quad (6)$$

When actually performing hydro-bulge forming, the maximum pressure read from the meter of the manual hydraulic pump was 2.2 MPa. This shows that it was 7.84% higher than the water pressure value at the onset of plastic deformation calculated using Equation (6). This is believed to be caused by the effect of the work hardening of the sidewall material during the hydro-bulge forming process.

Equation (5) indicates that the water pressure required for forming is proportional to the relative plate thickness, which is the ratio of plate thickness to the radius of the spherical tank; larger relative radii of the spherical tank require lower water pressures.

4.3. Spring-Back After Forming

Unlike the conventional method of welding and assembling prefabricated curved parts, spring-back occurs in the hydro-bulge forming method when the internal water

pressure is removed after plastic deformation. Accurate analysis of the spring-back effect on the molded shape is complicated. Here, we predicted this using a simple method.

Considering the symmetry of the spherical tank, only the effect of spring-back on the spherical tank must be considered by reducing its radius. The strain generated in the circumferential direction owing to spring-back after formation can be calculated using the following equation.

$$\varepsilon = \frac{2\pi R - 2\pi(R - \Delta R)}{2\pi R} = \frac{\Delta R}{R} = \frac{\sigma}{E} \quad (7)$$

where E is Young's modulus of the material. Here, the tensile stress of the sidewall is replaced with the yield stress for the evaluation. Based on the molding experiment example in the previous section, a yield stress of 255 MPa and Young's modulus of 193 GPa for stainless steel SUS304 were substituted in Equation (7). The relative radius reduction of the spherical tank caused by spring-back is estimated using the following equation.

$$\frac{\Delta R}{R} = \frac{255 \times 10^6}{193 \times 10^9} = \frac{1.3}{1000} = 0.13\% \quad (8)$$

From Equation (8), the radius reduction caused by spring-back was considerably small. A radius of 500 mm was considered to be reduced by approximately 0.65 mm because of spring-back.

However, using the yield stress instead of the actual plastic deformation stress causes an error when using Equation (7). Considering this, we can predict the range of radius change caused by spring-back using Equation (8).

5. Conclusion

In this study, we proposed a soccer-ball-shaped spherical tank and integrated hydro-bulge forming method. After confirming the forming performance using the FEM, a formation experiment was conducted for a spherical tank with a diameter of 500 mm. After a detailed examination, the following conclusions were drawn.

The proposed forming method does not require a press forming process because only regular hexagonal and pentagonal plate parts must be cut from a flat steel plate. Welding along the edges of the hexagonal and pentagonal parts naturally forms a soccer ball, thereby eliminating the need for positioning jigs. This improves the molding shape accuracy.

The experiment results confirmed that the shape accuracy of the formed spherical tank was high because the expansion force of the internal water pressure was completely symmetrical. The roundness of the soccer ball-shaped tank with a diameter of 500 mm was 2.36 mm.

A design formula using $a = 0.4 R$ for regular hexagonal and pentagonal plate parts was derived. In the molding experiment, a plate with a side length of 100 mm was designed with a target radius of 250 mm. The measured radius of the molded spherical tank was 249.26 mm. Thus, the accuracy of the

design formula was verified.

A formula for calculating the internal water pressure required for hydro-bulge formation was derived. The internal water pressure was determined to be proportional to the relative plate thickness, which is the ratio of the plate thickness to the radius of the spherical tank. The water pressure in the formation experiment and calculated values almost matched.

After hydro-bulging, the relative radius reduction of the spherical tank caused by spring-back is small; it can be predicted using the ratio of the yield stress to the Young's modulus of the material. The formation experiment used a SUS304 stainless steel plate with a thickness of 1.0 mm, and the prediction result revealed that it was reduced by approximately 0.65 mm with respect to a radius of 500 mm.

Large-scale press machines and complicated positioning jigs are not required when using the proposed hydro-bulge forming method. It has the advantages of a high formation accuracy and low energy requirements. This contributes to the future development of practical applications.

References

- [1] Oyelami, A. T., & Olusunle, S. O. O. (2019). Spherical Storage Tank Development Through Mathematical Modeling of Constituent Sections. *Mathematical Modelling of Engineering Problems*, 6 (3), 467-473. doi.org/10.18280/mmep.060320.
- [2] Cheng, B., Huang, J. X., & Shan, Y. (2015). The Economic Design and Analysis for Mixed Model Spherical Tank Shell Angle Partition. *Procedia Engineering*, 130, 41-47. doi: 10.1016/j.proeng.2015.12.173.
- [3] Arabzadeh, V., Niaki, S. T. A., & Arabzadeh, V. (2018). Construction cost estimation of spherical storage tanks: artificial neural networks and hybrid regression—GA algorithms. *Journal of Industrial Engineering International*, 14, 747-756. doi.org/10.1007/s40092-017-0240-8.
- [4] Milovanović, A., & Sedmak, A. (2021). Integrity assessment of ammonia spherical storage tank. *Procedia Structural Integrity*, 13, 994-999. doi.org/10.1016/j.prostr.2018.12.185.
- [5] Rath, S., & Krol, M. (2013). Comparative Risk Assessment for Different LNG-Storage Tank Concepts. *Chemical Engineering Transactions*, 31, 103-108. doi.org/10.3303/CET1331018.
- [6] Ibrahim, A., Ryu, Y., & Saidpour, M. (2015). Stress Analysis of Thin-Walled Pressure Vessels. *Modern Mechanical Engineering*, 5 (1), 1-9. doi: 10.4236/mme.2015.51001.
- [7] Shin, S. H., & Ko, D. E. (2016). A study on forces generated on spherical type LNG tank with central cylindrical part under various static loading. *International Journal of Naval Architecture and Ocean Engineering*, 8 (6), 530-536. doi.org/10.1016/j.ijnaoe.2016.07.001.
- [8] Pan, B., & Cui, W. (2010). An overview of buckling and ultimate strength of spherical pressure hull under external pressure. *Marine Structures*, 23, 227-240. doi: 10.1016/j.marstruc.2010.07.005.
- [9] Adeyefa, O., & Oluwole, O. (2011). Finite Element Analysis of Von-Mises Stress Distribution in a Spherical Shell of Liquefied Natural Gas (LNG) Pressure Vessels. *Engineering*, 3, 1012-1017. doi: 10.4236/eng.2011.310125.
- [10] Adeyefa, O., & Oluwole, O. (2013). Finite Element Modeling of Shop Built Spherical Pressure Vessels. *Engineering*, 5, 537-542. doi: 10.4236/eng.2013.56064.
- [11] Kandure, R. S., & Lahoti, G. V. (2019). Design and Structural Analysis of Spherical Pressure Vessel used to Operate a Pneumatic Jack Hammer. *International Journal of Engineering Research & Technology*, 8 (9), 773-777. doi: 10.17577/IJERTV8IS090234.
- [12] Schrader, R. F. (1985). Method of constructing a large spherical tank supported by a skirt on land. United States Patent, US4522010A.
- [13] Arne, C. (1950). Spherical segment tank and method of making same. United States Patent, US2668634A.
- [14] Kvamsdal, R., & Tobiassen, R. (1976). Ships for transport of liquefied gases. United States Patent, US3968764A.
- [15] Mehrasa, H., Liaghat, G., & Javabvar, D. (2012). Experimental analysis and simulation of effective factors on explosive forming of spherical vessel using prefabricated four cones vessel structures. *Central European Journal of Engineering*, 2, 656-664. doi.org/10.2478/s13531-012-0036-y.
- [16] Suzuki, T., & Takenaka, N. (1975). Method of constructing a spherical tank or the like. United States Patent, US3921555A.
- [17] Brinkman, H. C. (1942). Storage tank. United States Patent, US2295514A.
- [18] Anttila, J., Gustafsson, J., Heinakari, M., Linja, J., & Vaihinien, M. Spherical lng-tank and a production method for such a tank. United States Patent, US5529239A.
- [19] Baysinger, F. R. (1980). Liquefied natural gas tank construction. United States Patent, US4181235A.
- [20] Yuan, S., & Fan, X. (2019). Developments and perspectives on the precision forming processes for ultra-large size integrated components. *International Journal of Extreme Manufacturing*, 1 (2), 022002. doi.org/10.1088/2631-7990/ab22a9.
- [21] Yuan, S. (2021). Fundamentals and Processes of Fluid Pressure Forming Technology for Complex Thin-Walled Components. *Engineering*, 7, 358-366. doi.org/10.1016/j.eng.2020.08.014.
- [22] Bell, C., Corney, J., Zuelli, N., & Savings, D. (2020). A state of the art review of hydroforming technology. 13, 789-828. doi.org/10.1007/s12289-019-01507-1.